We are IntechOpen, the world's leading publisher of Open Access books Built by scientists, for scientists

6,300
Open access books available

171,000
International authors and editors

190M
Downloads

Our authors are among the

154
Countries delivered to

TOP 1%
most cited scientists

12.2%
Contributors from top 500 universities

CLARIVATE ANALYTICS
BOOK CITATION INDEX
INDEXED

WEB OF SCIENCE™

Selection of our books indexed in the Book Citation Index
in Web of Science™ Core Collection (BKCI)

Interested in publishing with us?
Contact book.department@intechopen.com

Numbers displayed above are based on latest data collected.
For more information visit www.intechopen.com

Chapter

The Role of Optical Coherence Tomography Angiography in Glaucoma

Karanjit Kooner, Mahad Rehman, Sruthi Suresh,
Emily Buchanan, Mohannad Albdour and Hafsa Zuberi

Abstract

Glaucoma is the second leading cause of blindness worldwide, affecting eighty million people globally and three million patients in the USA. Primary open-angle glaucoma, the most common type, is a multifactorial progressive optic nerve neurodegenerative disorder that leads to loss of optic nerve head (ONH) tissue, thinning of the retinal nerve fiber layer, and corresponding visual field (VF) defects with or without elevated intraocular pressure (IOP). Risk factors include older age, black or Hispanic race, elevated IOP, thin central corneal thickness, disk hemorrhage, and low ocular perfusion pressure. The two prevalent theories explaining glaucomatous damage are mechanical (elevated IOP) and vascular (compromised optic nerve perfusion). Current diagnostic methods, such as measuring IOP, VF testing, and ONH evaluation, are subjective and often unreliable. Optical coherence tomography angiography (OCTA) is a rapid, non-invasive imaging modality that provides 3-D, volumetric details of both the structure and vascular networks of the retina and optic nerve. Various researchers have shown that OCTA provides an accurate and objective evaluation of the retina and the optic nerve in glaucoma. This chapter describes the role of OCTA in managing patients with glaucoma.

Keywords: optical coherence tomography angiography, glaucoma, intraocular pressure, optic nerve, visual field

1. Introduction

1.1 Overview of glaucoma

Glaucoma is the second leading cause of blindness which affects over 80 million people worldwide [1]. Of the various subtypes of glaucoma, the most common is primary open-angle glaucoma (POAG), a multifactorial, progressive optic neuropathy characterized by cupping of the optic nerve head (ONH) and visual field (VF) defects with or without elevated intraocular pressure (IOP) [2]. Glaucomatous optic neuropathy is driven pathologically by degeneration of the retinal ganglion cells (RGCs) and atrophy of the retinal nerve fiber layer (RNFL), **Figure 1**.
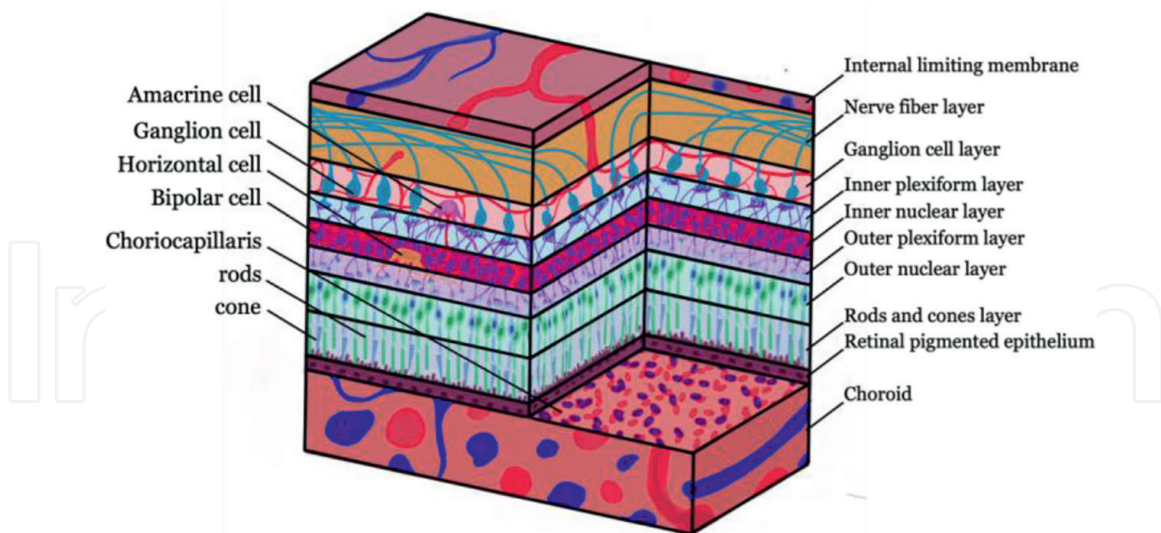
Figure 1.
Cross-section of the retina illustrating the retinal layers and underlying vascular supply in a healthy eye.

Early work in 1858 by German anatomist Heinrich Mueller led to the concept of the mechanical theory: elevated IOP leads to the compression of optic nerve fibers at the level of the lamina cribrosa which in turn causes blockages to the axoplasmic flow [3]. In the same year, another German scientist, Eduard von Jaeger proposed an alternative vascular theory where he suggested that the underlying cause of optic nerve damage was due to poor perfusion to the ONH with or without elevated IOP [4]. Today, it is widely accepted that glaucoma being a multifactorial disease may be consistent with both the mechanical and vascular models. Schematics in **Figures 2** and **3** show the pathological changes a human eye undergoes during glaucoma as per the vascular and mechanical theories.

1.2 Optical coherence tomography angiography addresses current challenges in glaucoma diagnosis

Glaucoma is diagnosed using three parameters: measurement of IOP, evaluation of the optic nerve anatomy, and VF testing. However, this approach is limited by its inherent subjectivity and measurement inconsistencies. One key challenge is that IOP measurement is not standardized and can be affected by the central corneal thickness (CCT), type of tonometer used, time of day, as well as the skill and training of the clinical staff obtaining the measurements. Similarly, visual assessment of the optic nerve and VF testing are subject to high degrees of inter- and intra-examiner variation, limiting their abilities to diagnose and follow patients with glaucoma accurately and objectively.

Due to these challenges, optical coherence tomography (OCT) technology has grown in popularity due to its ability to provide additional objective information about the structure and morphology of the optic nerve and retina. Specifically, peripapillary retinal nerve fiber layer (RNFL) analysis is widely used for glaucoma diagnosis, as RNFL thinning can indicate glaucomatous damage [5]. While OCT has greatly improved the accuracy and consistency of glaucoma diagnosis, it is still limited since it cannot probe the vascular degradation that occurs in glaucoma. Particularly, it is extremely challenging to distinguish between differing degrees of glaucoma severity, identify patients with optic cupping who have normal vascular perfusion, as well as monitor patient response to treatment over time.
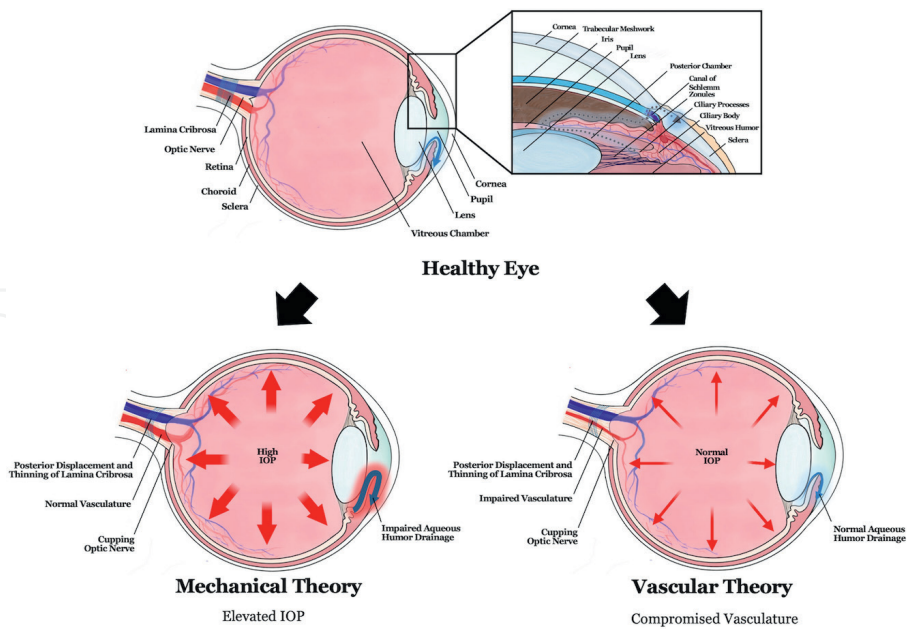
Figure 2.
Aqueous humor dynamics in the healthy (top) and glaucomatous (bottom) eye as hypothesized by the mechanical theory (left) and vascular theory (right).
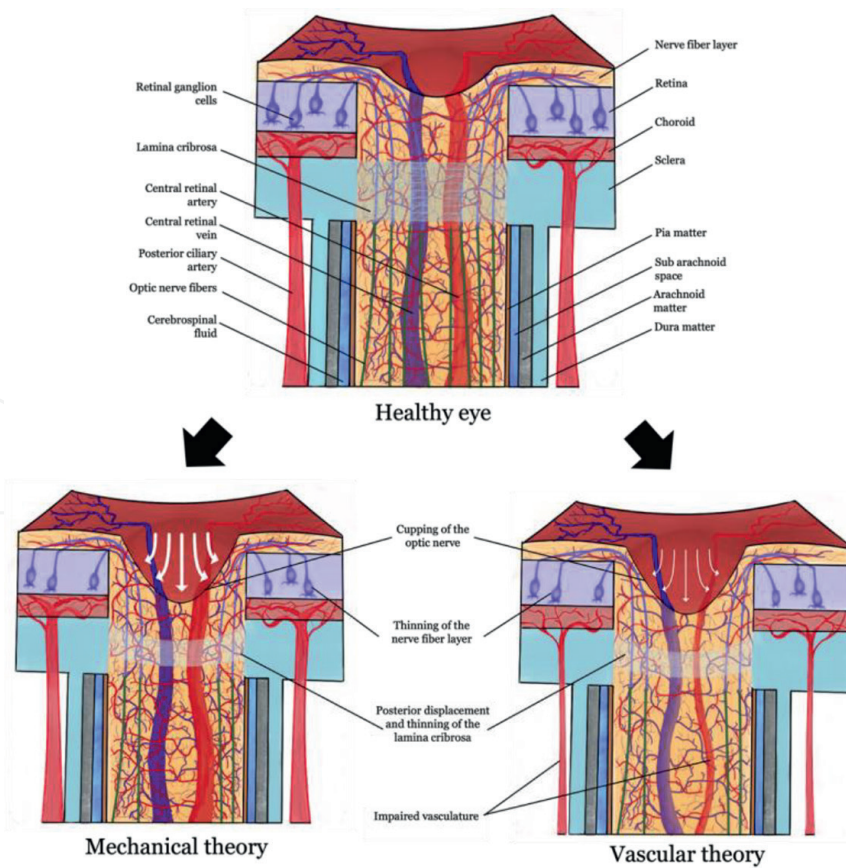

Figure 3.
Cross section of the optic nerve in the healthy (top) and the glaucomatous (bottom) eye as hypothesized by the mechanical theory (left) and vascular theory (right).

Improvements in the OCT technology has led to the development of optical coherence tomography angiography (OCTA), a rapid, noninvasive imaging modality that can provide quantitative and volumetric assessment of both the structure and vascular aspects of the retinal and optic nerve. Thus, OCTA has addressed prior limitations of OCT and has revolutionized the evaluation of several ophthalmic diseases, including glaucoma by allowing clinicians to distinguish between glaucoma suspect, healthy, and glaucomatous eyes [6–9].

2. Optical coherence tomography angiography

2.1 The development of optical coherence tomography

OCT technology was first developed at the Massachusetts Institute of Technology by David Huang in 1991 [10] (**Figure 4**). It is a non-invasive imaging methodology for acquiring high resolution images of the retina and optic nerve using low-coherence interferometry. In this technique a beam of light is shone into the eye and reflected light is captured and measured. By comparing the reflected light to an unobstructed reference path, the location and morphology of ocular structures can be determined to generate a cross sectional image of the eye [10, 25]. This imaging modality provides key structural information such as retinal thickness (μm), RNFL thickness (μm), and abnormal reflectivity on retinal layers which could indicate the presence of edema, exudates, calcifications, or atrophy [26, 27]. Thus, OCT technology introduced a novel and precise method for visualizing and measuring defects in the optic nerve, retina, and nerve fiber layer. Soon after the publication of the first images of the optic disk, Humphrey instruments introduced the first commercial OCT scanner in 1996 [11]. Ten years later, Optovue's spectral domain (SD-OCT) scanner was the first to obtain FDA approval for clinical use [12].
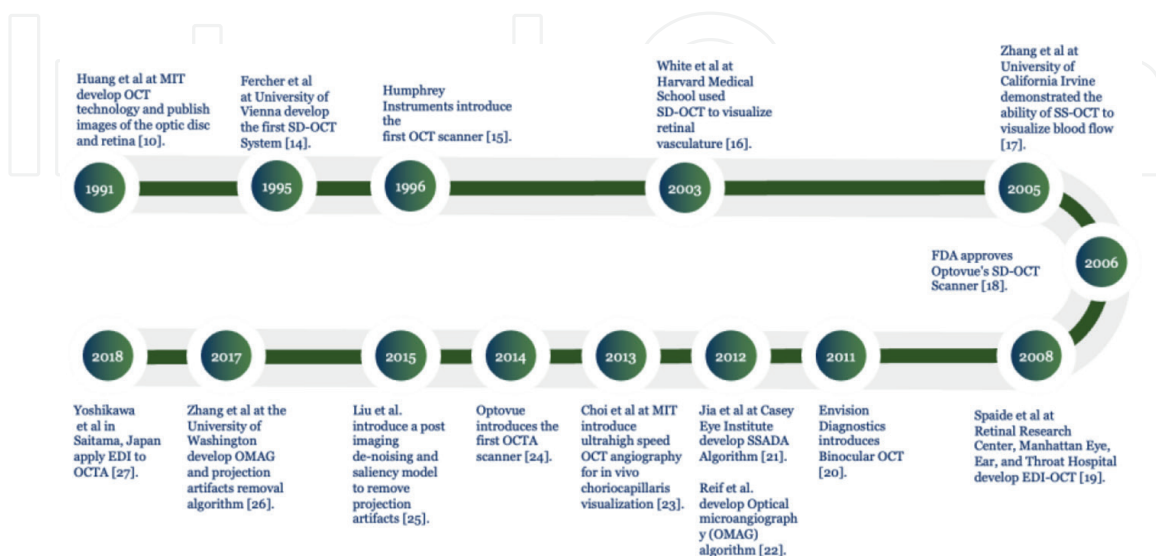

Figure 4.
Milestones in the development of optical coherence tomography angiography [10–24].

2.2 The development of optical coherence tomography angiography

Although OCT can provide information about the structure of the retina and the optic nerve, it is unable to assess the vascular impairment and degradation known to play a key role in glaucoma pathophysiology. To fully assess damage in glaucoma patients, additional details about the retina and optic nerve vasculature are needed.

Initial work by White et al. showed that SD- OCT could be used to probe the retinal vasculature and was expanded upon by Zhang et al. who used a technique called swept source (SS) OCT to visualize blood flow in 2005 [14, 15]. This was accomplished by repeatedly scanning a transverse cross-sectional area of the retina and analyzing the scan differences caused by movement [6]. Since the presence of blood flow creates movement which affects the reflectance in each scan, successive scans or "angiograms" can be used to probe the underlying vasculature of the eye.

In 2018, Nesper et al. demonstrated the complexity and connectivity of parafoveal capillary plexuses and identified the location of specific arterioles seen in prior histological studies [28]. This enhanced understanding of vasculature and their perfusion greatly improved the assessment of many ophthalmological diseases, including glaucoma.

Work in the past decade has focused on accurately delineating blood vessels by employing sophisticated algorithms. In 2012 Reif et al. introduced a phase-based algorithm known as optical microangiography (OMAG), which uses intensity and phase information from repeated B-scans to delineate blood vessels [19]. In the same year, Spaide et al. showed that an amplitude-based method called split-spectrum amplitude decorrelation angiography (SSADA) could delineate blood vessels by measuring the decorrelation between two consecutive B-scans [6]. Research has found SSADA to be superior in the detection and connectivity of microvascular networks compared to other algorithms [18]. Current investigations of OCTA technology aim to implement novel deep learning (DL) and machine learning (ML) techniques to reduce or remove image artifacts to enhance OCTA accuracy.

3. Optical coherence tomography angiography in glaucoma

3.1 Optical coherence tomography angiography metrics for glaucoma evaluation

Early OCTA work in glaucoma by Jia et al. in 2012, was limited to the observation and quantification of the optic disk alone (disk flow index and disk perfusion) [29]. As this technology has progressed, a broad range of OCTA metrics were introduced to quantify microvasculature and aid in the diagnosis of glaucoma. Specifically, density parameters are used to track disease progression [18, 30–33] and more recent work has explored how changes in the macular regions, foveal avascular zone (FAZ), and deep retinal layer microvasculature contribute to disease severity [9].

Current clinical evaluations of glaucoma using OCTA rely predominantly on eight parameters: RNFL (µm), cup/disk ratio (CDR), macular ganglion cell complex (mGCC) in µm, focal loss volume (FLV, %), global loss volume (GLV, %), whole image ONH vessel density (VD, %), whole image macular VD, (%), and FAZ area (mm^2). Recently, a key study by AlSalem et al. explored the efficacy of each of these metrics for classifying the severity of glaucoma progression into three categories: mild, moderate, severe [9]. Their parameter classifications are summarized in **Table 1**. Of note, the authors described how severe cases of POAG showed a

Variables	Controls (n = 69) (%)	Mild Glaucoma (n = 54) (%)	Moderate Glaucoma (n = 25) (%)	Severe Glaucoma (n = 12) (%)	P value* (All groups)
RNFL (μm)	96.11 ± 9.80	82.95 ± 11.75	76.91 ± 14.45	60.13 ± 7.51	<0.01
CDR	0.49 ± 0.14	0.54 ± 0.15	0.57 ± 0.17	0.73 ± 0.12	<0.01
mGCC Average (μm)	94.29 ± 9.65	83.71 ± 8.65	80.31 ± 14.99	67.92 ± 10.90	<0.01
FLV (%)	1.08 ± 1.21	2.93 ± 3.46	6.12 ± 3.92	9.39 ± 4.03	<0.01
GLV (%)	4.53 ± 4.78	12.37 ± 7.82	17.05 ± 11.31	29.39 ± 8.89	<0.01
Whole Image ONH Vessel Density (%)	56.71 ± 4.36	52.85 ± 5.15	49.82 ± 4.06	43.12 ± 4.19	<0.01
Whole Image Macular Vessel Density (%)	50.27 ± 4.23	48.12 ± 3.80	46.13 ± 3.91	43.43 ± 4.71	<0.01
FAZ Area (mm^2)	0.34 ± 0.14	0.33 ± 0.14	0.40 ± 0.16	0.36 ± 0.16	0.51

Table 1.
Structural and vessel density characteristics of healthy controls and glaucomatous eyes, adapted from AlSalem et al. [9].

significant decrease in signal strength intensity (SSI) for RNFL and ONH VD scans, whereas four parameters (whole image ONH VD, whole image macular VD, average RNFL thickness, and average mGCC thickness) decreased in a stepwise fashion as glaucoma progressed. These findings enable researchers to use both structural and VD parameters as indicators of glaucoma severity, adding new prognostic metrics that could not be obtained through VF tests alone.

3.1.1 Optical coherence tomography angiography features of the optic nerve head in glaucoma

Evaluation of the ONH microcirculation is commonly used to detect vascular damage in the glaucomatous eye, as there is a significant correlation between glaucoma severity and degree of VD loss in this region [9]. While the ONH of a healthy eye displays a dense microvascular network with no focal capillary dropout and a full RNFL thickness, the ONH microcirculation of a glaucomatous eye shows decreased perfusion and loss of the RNFL [9, 18].

In 2012, Jia et al. developed the SSADA algorithm to visualize and quantify ONH microcirculation [18]. In this pilot study, the SSADA results were applied to patients with early glaucoma to detect ONH perfusion abnormalities. The researchers found that ONH flow index and VD in patients with early glaucoma were significantly reduced compared to healthy controls. Furthermore, the ONH perfusion defects preceded VF changes, aiding in the early detection of disease.

Four years later, Chen et al. used OMAG-based OCTA to evaluate ONH blood vessels and perfusion and found that ONH perfusion decline was significantly correlated to the presence of structural and functional defects as well as disease severity [30]. Recently, Eslami et al. showed that OCTA ONH parameters can also discriminate between stages of glaucoma. Their cross-sectional investigation of patients with moderate and advanced glaucoma found that the VD of the inferior hemifield of the ONH area had the best performance in discriminating POAG stages [33].

3.2 Optical coherence tomography angiography features of the peripapillary region in glaucoma

Compared to healthy eyes, glaucomatous eyes show significantly lower peripapillary VD and blood flow index. A systematic review conducted by Bekkers et al. determined that the peripapillary microvasculature zone was the most discriminative region to aid glaucoma diagnosis as it provided an area under receiver operator characteristic curve AUROC of 0.8. [32]. Further gains in AUROC were obtained when model parameters were constricted to the superficial capillary plexus within the peripapillary region (AUROC =0.87).

Later work by De Jesus et al. confirmed that the superficial layer of the peripapillary region was the most useful OCTA metric to discern a glaucoma diagnosis, as damage was most prominent in this zone of the eye when compared to healthy controls [31]. Thus, analyzing the peripapillary region is a powerful application of OCTA as it provides the highest discriminant power to differentiate between healthy and glaucomatous eyes.

3.3 Optical coherence tomography angiography features of the macula in glaucoma

The macula is an area of great interest in glaucoma since it contains the highest density of RGCs. These multilayered cells are believed to be damaged early in the disease process [34]. Not only does a correlation exist between mean macular thickness and VF sensitivity, but the macular region has also been shown to have a significantly lower VD and blood flow index in patients with glaucoma compared to healthy controls [31].

In an age-matched study, Takusagawa et al. assessed macular thickness and circulation in patients with preperimetric glaucoma (PPG) and found that they had significant macular perfusion defects compared to healthy controls [35]. The authors additionally found that within the macular region, the hemispheric superficial vascular complex (SVC) VD values were highly correlated with the corresponding GCC thickness and VF sensitivity in glaucoma patients. Their landmark findings indicate that early in the disease process, glaucoma preferentially affects perfusion in the SVC of the macula rather than the deeper plexuses.

3.4 Optical coherence tomography angiography features of the choroidal microvasculature in glaucoma

According to vascular theory, changes in the choroidal microvasculature may play a key role in the pathophysiology of glaucoma as it supplies nutrition to both the optic nerve and the outer layers of retina. In a study evaluating parapapillary choroidal microvasculature dropout (MVD), Kim et al. found that MVD was associated with progressive RNFL thinning and worsening VF parameters [36]. The authors proposed that progressive retinal ganglion cell damage decreases metabolic demand and leads to reduced vascular perfusion and more extensive MVD.

Recently, Chatziralli et al. found that the peripapillary and MVD were lower in eyes with pseudoexfoliative glaucoma (PXG) [37]. This indicates optic nerve hypoperfusion may play a greater role in patients with PXG.

3.5 Using optical coherence tomography angiography to monitor disease progression in glaucoma

OCTA may have a role in the early detection and monitoring of the progression of glaucoma progression. AlSalem et al. found that whole image ONH VD, whole image macular VD, average RNFL thickness, average mGCC thickness, and cataract status were predictive of worsening VF MD [9]. They also determined that structural properties and VD were equally effective at determining the glaucomatous stage. This was supported by the findings of Geyman et al. and Chen et al. who also determined that structural properties and VD values were equally effective at determining the glaucoma stage [38, 39]. Tracking the previously described OCTA parameters over time may enable physicians to objectively gauge glaucoma progression.

3.6 Use of optical coherence tomography angiography in healthy, glaucoma suspect, and eyes with POAG

Using a standard OCTA protocol, typical qualitative and quantitative findings in healthy, glaucoma suspects, and eyes with POAG are shown in **Figure 5**. A, E, and I are images of the ONH and corresponding CDR. The B, F, and J show a map of the superficial retinal vessels and VD in different zones around the macula. C, G, and K show the nerve fiber layer thickness in the corresponding zones. D, H, and L are area maps of the radial peripapillary capillary VD.

The healthy eye (5A-D) has normal retinal morphology and OCTA parameter values. The CDR is 0.35, the retinal VD is 46%, the RNFL thickness is 113 μm, and the peripapillary capillary density is 53%. In a glaucoma suspect eye (5E-H), the enlarged CDR (0.80) alone may mislead the clinician. However, OCTA measurements of the VD (43%), RNFL (115 μm), and peripapillary capillary density (54%) are in the normal range. The OCTA scans of an eye with POAG (5I-L) show several abnormal findings characteristic of glaucoma. There is a severe degree of cupping (CDR 0.85), the overall retinal VD is reduced to 34%, the RNFL thickness is 55 μm, and the radial peripapillary VD is 34%.
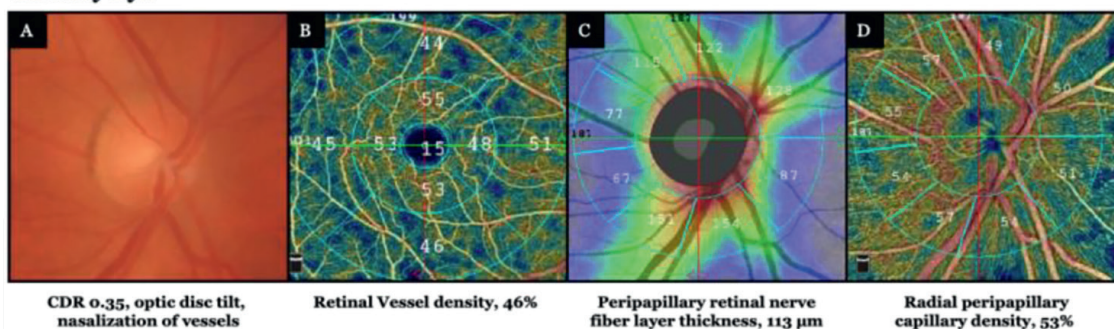
3.7 Using optical coherence tomography angiography to characterize myopia

In clinical practice, detecting glaucoma in myopic patients has always been extremely challenging. As myopia increases, findings such as ONH tilt, increased ovality of the ONH, and peripapillary atrophy become more prominent [40]. The peripapillary RNFL thickness peaks also shift in myopic eyes, leading to difficulties in detecting thinning (40. Examples of changes seen in a patient with moderate myopia are shown in **Figure 6**.
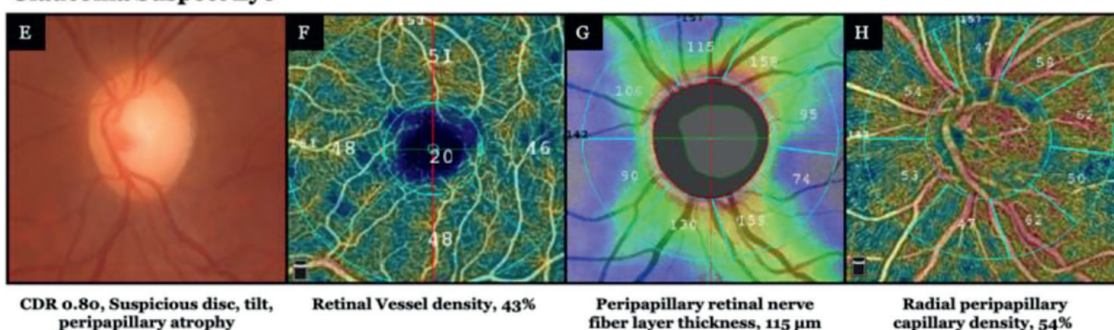
In patients with high myopia, OCTA can be helpful in identifying the narrowing of vessel diameters which leads to reduced retinal VD and indirectly implying impaired blood flow. Suwan et al. found that patients with myopia alone had lower peripapillary VD compared to healthy controls [41]. Furthermore, patients with both myopia and glaucoma had an even greater reduction in VD that allowed the researchers to distinguish these patients from healthy controls, myopia only patients, and patients with glaucoma alone [41].

Recent work by Chang et al. found that both peripapillary and macular perfusion density were significantly reduced in patients with high myopia (HM) compared to non-high myopic (NHM) healthy controls [42]. However, macular perfusion

Healthy Eye

| CDR 0.35, optic disc tilt, nasalization of vessels | Retinal Vessel density, 46% | Peripapillary retinal nerve fiber layer thickness, 113 μm | Radial peripapillary capillary density, 53% |

Glaucoma Suspect Eye

| CDR 0.80, Suspicious disc, tilt, peripapillary atrophy | Retinal Vessel density, 43% | Peripapillary retinal nerve fiber layer thickness, 115 μm | Radial peripapillary capillary density, 54% |

POAG Eye

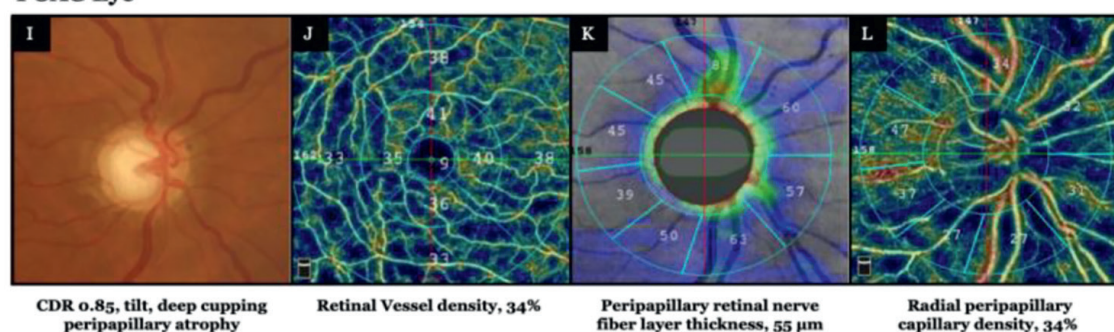| CDR 0.85, tilt, deep cupping peripapillary atrophy | Retinal Vessel density, 34% | Peripapillary retinal nerve fiber layer thickness, 55 μm | Radial peripapillary capillary density, 34% |

Figure 5.
Comparison of OCTA scans in healthy, glaucoma suspect, and eyes with POAG captured using the RTVue XR Avanti scanner (SSADA algorithm).
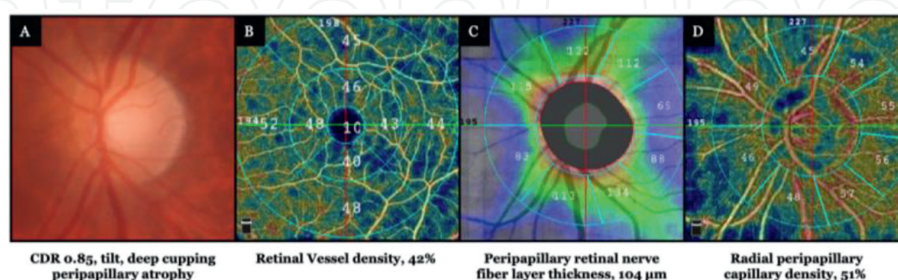

| CDR 0.85, tilt, deep cupping peripapillary atrophy | Retinal Vessel density, 42% | Peripapillary retinal nerve fiber layer thickness, 104 μm | Radial peripapillary capillary density, 51% |

Figure 6.
OCTA scans from a non-glaucomatous myopic eye captured using the RTVue XR Avanti scanner (SSADA algorithm).

density was not decreased between patients with and without HM and could not be used for accurate diagnosis. They recommended that both macular OCTA and OCT imaging may be useful in diagnosing early glaucoma in patients with myopia. Shin et al. showed that peripapillary VD correlated more with VF mean sensitivity than

peripapillary RNFL thickness and peripapillary perfusion density was significantly lower in patients with high myopia [43].

Bowd et al. took a different approach and created a novel *en face* texture-based analysis method to accurately discriminate between highly myopic glaucomatous and healthy eyes using macular tissue thickness measurements [40]. Their success was most likely due to the minimal tissue segmentation required in their approach compared to prior multilayer segmentation methods that often fail in highly myopic eyes. Another method by Yilmaz et al. found that utilizing a myopic normative database for peripapillary RNFL was very helpful in assessing differences in patients with varying degrees of myopia or when glaucoma co-existed with myopia [44]. Altogether, these recent works indicate that OCTA technology may improve the accuracy of glaucoma detection in patients with high myopia.

4. Limitations of optical coherence tomography angiography

Image artifacts are frequently encountered in OCTA and can hinder the interpretability of the microvascular structure and VD. In addition, media opacities and pupillary size can similarly affect the quality of OCTA maps and the calculation of VDs. Optimizing interscan time can also present a challenge in OCTA. While short capture times cannot detect slow flow velocities such as those observed in cases of venous occlusions [45], long interscan times are more sensitive to motion artifacts. Lastly, the lack of standardization across different devices and protocols remains a lingering limitation. For example, different commercially available OCTA devices differ in their methods of segmentation of the angiography slabs and axial and lateral resolutions [46].

4.1 Image artifacts in optical coherence tomography angiography

Image artifacts may be the result of errors during image acquisition, processing, and analysis and may be either patient related (**Figure 7**) or machine/operator related (**Figure 8**) [46].

4.1.1 Patient-related motion artifacts

One common cause of image artifacts is from eye movements caused by breathing, palpitations, or tremors (**Figure 7**). In general, eye movement artifacts appear as thin horizontal or vertical white lines (7A). They may cause duplication or removal of the retinal vessels shown in the image leading to an overall loss of vessel integrity. Blink
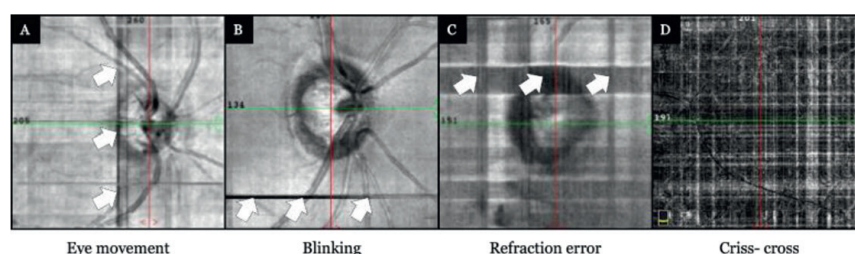

Figure 7.
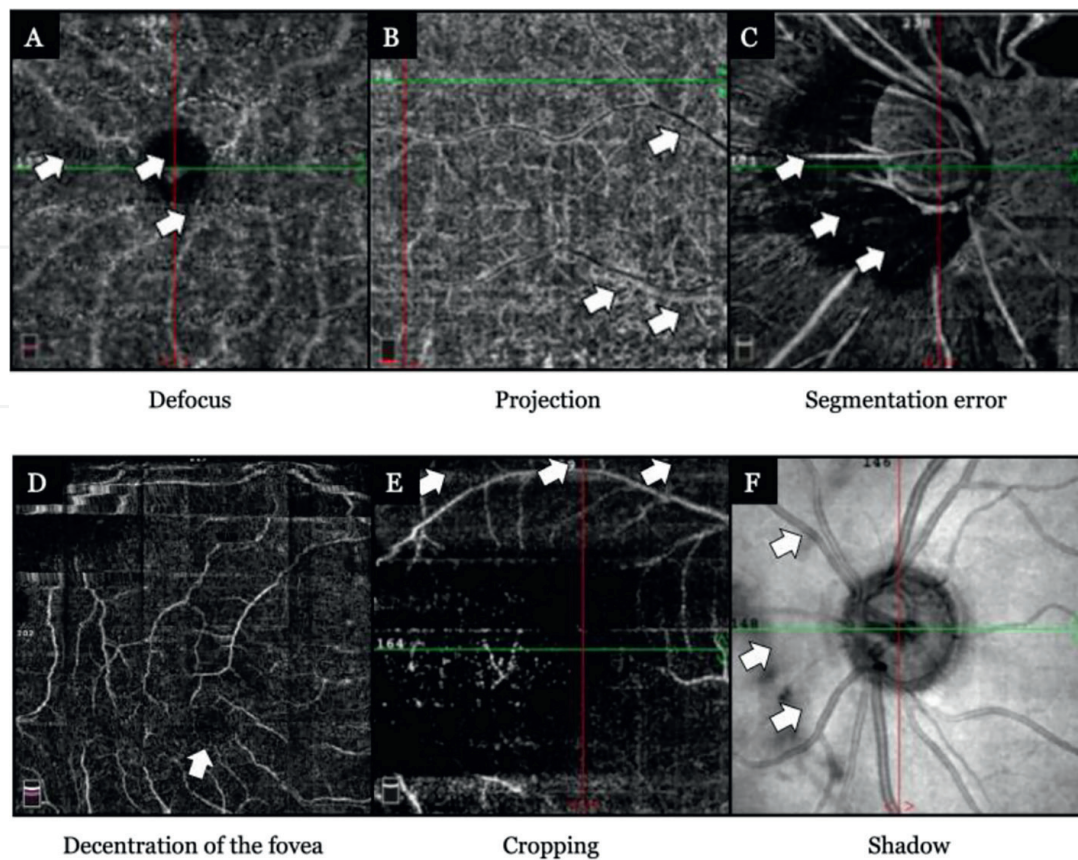*Examples of patient related motion artifacts.*

Figure 8.
Examples of operator or motion related OCTA artifacts.

artifacts occur when a patient blinks during scan capture which causes loss of reflectance intensity in an area of adjacent B-scans (7B). The displacement of multiple B-scans can cause horizontal or vertical black lines on the *en-face* angiogram. Refraction error, also described as banding, is caused by a temporary change in corneal refractive power when the patient-device distance fluctuates during acquisition (7 C). Criss-cross is an eye movement artifact that appears as a rectangular pattern when the software fails to correct multiple saccades (7D).

4.1.2 Operator/machine-related motion artifacts

There are several operator/machine related artifacts that affect the accuracy and precision of OCTA measurements. Poorly focused images cause defocused artifacts (8A) that are caused by a decrease in reflective intensity resulting in reduced definition of retinal microvasculature Projection artifacts (8B) occur when the shadow of vessels in the superficial layer imprint onto the deeper layer. Segmentation errors (8C) are produced when the automated segmentation algorithm inaccurately identifies the layers of the retina or optic nerve. Decentration artifact (8D) occurs if the fovea or ONH is translocated to the periphery of the scan, preventing the algorithm from correctly identifying these areas. Cropping (8E) refers to loss in image data caused by B-scan not being fully within the capture window. Lastly, vitreous floaters may result in shadow artifacts (8F) because of decreased intensity of retinal layers in focused areas and may prevent clear visualization of structures in the affected area.

4.1.3 Key factors that produce optical coherence tomography angiography artifacts

Since OCTA artifacts may affect the accuracy of glaucoma diagnosis it is important to understand when and why these alterations are likely to occur. Older patients often have poor-quality scans due to a higher frequency of media opacities such as cataracts and age-related retinal pathologies. Recently Kamalipour et al. showed that 40% of OCTA images in the glaucoma group had poorer quality compared to healthy controls [47]. This was confirmed by Cheng et al. who found that the presence of glaucoma significantly increased the odds for the presence of any artifacts [48]. Similarly, patients with glaucoma were found to have two times the odds of incorrect automatic segmentation of the retinal superficial layer even after adjustment for age and VF loss [48]. Image quality was also found to decrease as glaucoma progressed. Declining retinal thickness reduces the signal intensity of reflected waves causing increased prevalence of artifacts.

4.1.4 Prevalence of optical coherence tomography angiography artifacts

In a well-diversified population of North Texas consisting of 292 patients, Mekala et al. found that most patients (99.3%) had at least one artifact [49]. The most common artifacts were due to eye movements (66.1%), defocus (64.7%) and shadows (40%). The most severe (affecting more than 10% of the scan area) were seen in patients with POAG (31.4%) and myopia (30.75%). A similar study by Weijing et al. found that 88.34% of images had at least one artifact, the most common of which was projection (100%), followed by motion (75.22%), blur (24.78%) and decentration (21.28%) [50]. Another study by Kamalipour et al. excluded 33.9% of scans due to poor image quality and found that 13.6% had one artifact and 9.8% had two or more. In this study the most common artifact was eye movement (10.6%), followed by defocus (9.6%), correctable segmentation errors (7.6%), and uncorrectable segmentation errors (5.4%) [48]. Given that multiple studies have confirmed the presence of artifacts in a significant percentage of images, it is crucial to account for artifacts when evaluating OCTA in a clinical setting.

4.1.5 Current methods for reducing optical coherence tomography angiography artifacts

Eye tracking technology was first introduced in 2004 as a way to compensate for eye movement and improve the quality of OCT scans [51]. Since then, this technology has shown to decrease the odds of acquiring poor-quality images by half [47]. It is highly effective in reducing eye movement and defocus artifacts but does not currently decrease the occurrence of segmentation artifacts.

Work by Venugopal et al. found that high-density (HD) scans, which increase sampling density from 304 × 304 A-scans to 400 × 400 A-scans, showed significantly greater VD values and fewer poor-quality scans than non-HD scans [52]. Thus, both eye tracking technology and HD scanning are proven methods for reducing the presence of OCTA artifacts. However, additional work is needed to further reduce the prevalence of other artifacts in OCTA.

4.2 Repeatability and reproducibility challenges in optical coherence tomography angiography

OCTA's use is slowly becoming popular among clinicians for the diagnosis and monitoring of glaucoma. There are a number of commercially available OCTA devices

including RTVue XR Avanti (Visionix USA Inc., previously Optovue Inc., Lombard, IL), Cirrus 5000 (Carl Zeiss Meditec Inc., Dublin, CA), PLEX Elite 9000 (Carl Zeiss Meditec Inc., Dublin, CA), and SPECTRALIS 2 (Heidelberg Engineering, Heidelberg, Germany). These devices all vary in terms of scan speed, wavelengths, eye tracking, image size, and vessel delineation algorithms. Differences in scan parameters and methodologies have led to discrepancies between images that limit direct comparisons across multiple centers and studies.

Several investigators have evaluated intra and inter-visit repeatability and of OCTA measurements in the ONH, peripapillary, and macular regions. Manalastas et al. compared the reproducibility of VD measurements between healthy and glaucoma eyes using the coefficient of variation (CV) the relative dispersion of data points around the mean, with a lower number indicating less variation [53]. The authors found that the CV of intra- and inter-visit global VD measures in healthy eyes ranged from 2.5–9.0% in macular scans and 1.8–3.2% in ONH scans, while the CV was higher in glaucoma (3.2–7.9% in macular scans vs. 2.3–4.1% in ONH scans. Venugopal et al. described similar results for peripapillary region (normal 2.5–4.4% vs. glaucoma 2.6–6.6%) and macular region (normal 3.3–4.7% vs. glaucoma 3.7–5.6%) [51]. Together, these studies suggest that glaucoma patients have sparser VD with slightly poorer reproducibility than healthy subjects [52].

Manalastas et al. examined the intra-visit and inter-visit reproducibility of SD-OCT RNFL thickness and GCC thickness in the scans from the prior studies [53]. The CVs of the global RNFL and GCC thickness were $\leq 4\%$, and the superior and inferior RNFL and GCC $\leq 3.5\%$ in both healthy and glaucoma eyes. In agreement with the prior VD studies, glaucomatous eyes had worse RNFL and GCC reproducibility than healthy eyes ($p < 0.001$). The reproducibility of the global VD measures provided by OCTA is slightly worse than that of RNFL and GCC measures traditionally found in OCT.

AlSalem et al. studied reproducibility between patients across all stages of POAG and concluded that the range of CV for structural properties was greater than VD as glaucoma progressed [9]. Thus, as VD provides better reproducibility than structural values it may be a more consistent metric in severe POAG.

5. The future of optical coherence tomography angiography in glaucoma

Recently, artificial intelligence (AI) techniques such as machine learning (ML) and deep learning (DL) are increasingly being used in conjunction with OCTA to improve glaucoma diagnosis and track disease progression. However, further work is required to standardize the nomenclature and datasets utilized for ML and DL to maximize the impact of AI technology in OCTA.

5.1 Standardization of optical coherence tomography angiography

A major barrier that has prevented the compilation of large OCTA databases for ML and DL is the lack of standardization among OCTA instruments, imaging protocols, data analysis methods, and inconsistent nomenclature. This has made it very challenging to apply new technologies or methods to analyze data from different OCTA scanners and ophthalmology clinics. Therefore, establishing standardized protocols for imaging, data analysis, and terminology is crucial [54, 55].

5.2 Machine learning using optical coherence tomography angiography imaging

5.2.1 Overview of machine learning methodology

Broadly speaking, AI refers to computer science techniques which simulate human cognitive processes such as visual perception, speech recognition, and decision-making. ML is a subfield of AI that allows software systems to automatically learn and improve from experience without being explicitly programmed through the use of algorithms and statistical models that analyze and draw inferences from patterns in data. It involves training a model on a dataset and allowing the model to make predictions or decisions without human intervention [56, 57].

ML requires four sequential steps: an input of high-volume and high-quality data, extraction of features, model building, and performance evaluation [56]. The quality of the manual feature extraction from a dataset to be used as an input for ML is critical for optimal model performance. During this process, unique properties and patterns are identified which the model then uses to learn how to perform the task. These can include higher level features, such as glaucomatous eyes, or lower-level features such as image edges and shapes. The main caveat to high quality feature extraction is that it requires large data sets and many hours of precise identification of objects of interest by the researchers. One approach to reduce this burden is to use DL automated feature learning, where the model learns to extract and identify relevant features from a dataset automatically, without human intervention.

Once the features have been extracted and the model has been chosen, the next step is to train the model on a data set. During this process, the model's parameters are adjusted to minimize the error between the model's predictions and true value. The success of an ML model is usually evaluated in three categories: performance, resources required, and prediction accuracy [56]. Of these three, accuracy is perhaps the most important and difficult metric to assess because it requires an additional independent test dataset. The test dataset is given to the ML model and the predictions are compared against the true value or ground truth. If the model's performance is not satisfactory, it may be necessary to fine-tune the model by adjusting its hyperparameters or by training the model on additional data sets. Once the model has been trained and evaluated, it can be deployed to make predictions on new, unseen data.

5.2.2 Using machine learning for optical coherence tomography angiography analysis

Recently, ML image analysis methods have become an area of interest in OCTA research. Specifically, researchers aim to use AI to accurately detect pathology, precisely quantify retinal vasculature, and reliably diagnose disease [58]. In 2019, Chan et al. used features of the ONH and retina to automatically diagnose glaucoma from macular and disk images [59]. In this pilot study, the authors used the AdaBoost Classifier model, a self-adjusting classification tool. They reported excellent model accuracy of 94.3% on 109 images (57 normal, 52 glaucoma). This milestone study showed that ML could aid clinicians in glaucoma detection at an early stage.

In 2022, Kooner et al. developed an ML tool to identify the parameters which provided the most accurate diagnosis of glaucoma [60]. The authors analyzed six ML algorithms, and over 2500 ML models were optimized using random search. In this study, the XGBoost algorithm, a highly effective and scalable ML model, achieved

the highest accuracy of 83.9%. They also explored the ML decision tree models to understand the most useful diagnostic parameters (inferior temporal VD, inferior hemisphere VD, and peripapillary RNFL thickness).

5.2.3 Overview of deep learning methodology

DL is a subset of ML which uses artificial networks composed of "neurons" or nodes layered to resemble the human brain. DL algorithms can understand complex patterns and relationships in the data by adjusting the weights and biases of the connections between the neurons in the network. While DL architectures are more powerful learners than ML algorithms, they are less customizable and interpretable [56]. Additionally, DL models are very practical since they are able to automatically extract features from raw input data resulting in increased efficiency and pattern recognition. Convolutional neural networks (CNNs), a type of DL architecture specialized for image input data, are particularly useful for extracting features for DL training. They operate in a bottom-up manner, first identifying basic features such as corners and working up towards more complex structures. Similar performance metrics are utilized for both ML and DL models.

A disadvantage of DL is the need for a large volume of clinical data during the training process. This data acquisition process can be affected by privacy concerns and time constraints. DL tools which can be used to address this need for data are known as generative adversarial networks (GANs). GANs are a type of DL algorithm that are used for generating new, synthetic data that is similar to a given dataset. GANs are composed of two neural networks: a generator network, which is responsible for generating new data, and a discriminator network, which can distinguish the synthetic and real data. The goal of GANs is to generate synthetic data that is indistinguishable from real data, addressing issues posed in conventional data acquisition processes.

5.2.4 Using deep learning for optical coherence tomography angiography analysis

In recent years, the use of CNNs for automated glaucoma diagnosis has grown in popularity over prior ML techniques. In 2022, Bowd et al. used CNNs to improve the performance of feature-based gradient boosting classifier (GBC) analysis, an ML technique that combines multiple subsets of models to create a powerful classification tool, in 405 images (130 healthy, 275 glaucoma) [61]. GBC models were separately trained on OCT and OCTA scans of the ONH, while the CNN model was trained solely on region proposal classifier (RPC), a type of DL architecture used for object detection tasks. To account for the imbalance of healthy and glaucomatous eyes, areas under the precision recall curves (AUPRC) were computed to evaluate the performance of the two models. The CNN model had an AUPRC of 0.97, compared 0.93 for the best ML model, indicating that the DL models improve on feature-based ML models for classifying healthy and glaucomatous eyes.

In 2022 Kumar et al. used GANs to create synthetic OCT circumpapillary images, evaluate them for gradeability and authenticity, and use them to train DL models [62]. The researchers created two models to generate both healthy and glaucomatous synthetic OCT images of the circumpapillary ONH. The optimal DL network trained on synthetic images (AUC = 0.97 internal test data vs. 0.90 external test data), while the DL network trained with real images performed worse (AUC = 0.96 internal test data vs. 0.84 external test data). The accuracy of DL networks trained with synthetic

images were comparable to those trained with real images, indicating their potential use for other modalities such as OCTA and similar DL applications.

DL can also be used to enhance the quality of OCT and OCTA images affected by artifacts and speckle noise (noise caused by the coherent scattering of the light waves used to acquire the image). Early studies by Yamashita et al. used modified CNN tools to enhance the scan quality of noisy ONH OCTs [63]. Recently, Omodoka et al. denoised RPC OCTA images to improve the quality of calculated RPC vessel area density and vessel length density [64].

Since DL automated feature extraction acts like a "black box" concept, studies explaining DL decision making are vital. These "explainability" studies attempt to address the interpretability of DL, which will be crucial for clinical implementation. To better understand DL decision making, Hemelings et al. conducted a study on fundus images to determine the importance of the regions outside of the ONH for DL-based glaucoma detection and vertical CDR (VCDR) [65]. The researchers trained DL models on a database of 23,930 images and compared classification accuracy. They showed that models trained on the original unaltered images (AUC = 0.94, VCDR estimation = 77%) outperformed models that were trained on images with the absence of the ONH (AUC =0.80, VCDR estimation = 37%). Thus, these results provide evidence that DL models that use areas beyond the ONH, such as VCDR, are superior in classifying glaucomatous eyes.

6. Conclusion

Since the introduction of OCTA concept, the technology has increased the understanding of both the structural and vascular damage seen in patients with glaucoma. Not only is OCTA a safe, non-invasive, and quick test it provides the same structural information as OCT such as retinal and RNFL thinning, but it can also visualize relevant vascular parameters such as ONH VD and macular VD that typically undergo glaucomatous damage. However, significant limitations of OCTA such as a high prevalence of artifacts and lack of standardization across different machines currently do exist and must be accounted for while using this technology. Despite these limitations, the advantages of being able to observe both the structural and vascular damage caused by glaucoma show why OCTA is currently being adopted by ophthalmologists. In addition, the progress made in incorporating ML and DL techniques with OCTA will aid both in the diagnosis and progression in glaucoma.

Terminology

Disk perfusion: Refers to flow index and vessel density of the disk region.

Flow index: Average decorrelation values provided by the SSADA algorithm.

Focal loss volume (%): Describes the average focal loss of ganglion cells in the ganglion cell complex layer of the retina.

Global loss volume (%): Describes the average overall loss of ganglion cells in the ganglion cell complex of the retina.

Vessel density (%): Area occupied by blood vessels in any particular segment of the retina or ONH.

Vessel length density (%): Length of the vasculature divided by total image area.

Acknowledgements

Abbreviations

AI	Artificial intelligence
AUC	Area under the curve
AUPRC	Areas under the precision recall curves
AUROC	Area under receiver operator characteristic curve
CCT	Central corneal thickness
CDR	Cup/disk ratio
CNN	Convolutional neural network
CV	Coefficient of variation
DL	Deep learning
FAZ	Foveal avascular zone
GAN	Generative adversarial network
IOP	Intraocular pressure
LPQ	Local phase quantization
mGCC	Macular ganglion cell complex
ML	Machine learning
MVD	Microvascular dropout
NFL	Nerve fiber layer
OCT	Optical coherence tomography
OCTA	Optical coherence tomography angiography
OMAG	Optical microangiography
ONH	Optic nerve head
PCA	Principal component analysis
POAG	Primary open angle glaucoma
PPG	Preperimetric glaucoma
PXG	Pseudoexfoliative glaucoma
RGC	Retinal ganglion cell
RNFL	Retinal nerve fiber layer
RPC	Region proposal classifier
SSADA	Split-spectrum amplitude decorrelation angiography
SSI	Signal strength intensity
SVC	Superficial vascular complex
VCDR	Vertical cup/disk ratio
VD	Vessel density
VF	Visual field
VFMS	Visual field mean sensitivity

Author details

Karanjit Kooner[1,2*], Mahad Rehman[1], Sruthi Suresh[1], Emily Buchanan[1],
Mohannad Albdour[3] and Hafsa Zuberi[1]

1 Department of Ophthalmology, The University of Texas Southwestern Medical
Center, Dallas, Texas, USA

2 Veterans Affairs, North Texas Healthcare System, Dallas, Texas, USA

3 Department of Ophthalmology, King Hussein Medical Center, Amman, Jordan

*Address all correspondence to: karanjit.kooner@utsouthwestern.edu

IntechOpen

References

[1] Tham YC, Li X, Wong TY, Quigley HA, Aung T, Cheng CY. Global prevalence of glaucoma and projections of glaucoma burden through 2040: A systematic review and meta-analysis. Ophthalmology. 2014;**121**(11):2081-2090

[2] Gedde SJ, Vinod K, Wright MM, Muir KW, Lind JT, Chen PP, et al. Primary open-angle glaucoma preferred practice pattern®. Ophthalmology. 2021;**128**(1):71-150

[3] Müller H. Anatomische Beiträge zur Ophthalmologie. Archiv für Ophthalmologie. 1858;**4**(2):1-54

[4] Jaeger RV, Eduard J. Über Glaukom und seine Heilung durch Iridektomie. Z Ges Aerzte Wien. 1858;**30**:465-484

[5] Bussel II, Wollstein G, Schuman JS. OCT for glaucoma diagnosis, screening, and detection of glaucoma progression. Br J Ophthalmol. 2014;**98**(Suppl. 2): ii15-ii19

[6] Spaide RF, Fujimoto JG, Waheed NK. Optical coherence tomography angiography. Retina. 2015;**35**(11): 2161-2162

[7] Kumar RS, Anegondi N, Chandapura RS, Sudhakaran S, Kadambi SV, Rao HL, et al. Discriminant function of optical coherence tomography angiography to determine disease severity in glaucoma. Investigative Ophthalmology & Visual Science. 2016;**57**(14):6079-6088

[8] Yarmohammadi A, Zangwill LM, Diniz-Filho A, Suh MH, Manalastas PI, Fatehee N, et al. Optical coherence tomography angiography vessel density in healthy, glaucoma suspect, and glaucoma eyes. Invest Ophthalmol Vis Sci. 2016;**57**(9):451-459

[9] AlSalem M, Yang A, Noorani S, Deng T, Li X, Adams-Huet B, et al. Effectiveness of optical coherence tomography angiography (OCT-A) in staging glaucoma. Journal of the Royal Medical Services. 2022;**29**(2):1-15

[10] Huang D, Swanson EA, Lin CP, Schuman JS, Stinson WG, Chang W, et al. Optical coherence tomography. Science. 1991;**254**(5035):1178-1181

[11] Fujimoto J, Swanson E. The development, commercialization, and impact of optical coherence tomography. Invest Ophthalmol Vis Sci. 2016;**57**(9):Oct1-oct13

[12] Optovue Receives FDA. Clearance for Cornea/Anterior Module for RTVue. Company Website; 2006

[13] Fercher AF, Hitzenberger CK, Kamp G, El-Zaiat SY. Measurement of intraocular distances by backscattering spectral interferometry. Optics Communications. 1995;**117**(1):43-48

[14] White B, Pierce M, Nassif N, Cense B, Park B, Tearney G, et al. In vivo dynamic human retinal blood flow imaging using ultra-high-speed spectral domain optical coherence tomography. Optics Express. 2003;**11**(25):3490-3497

[15] Zhang J, Chen Z. In vivo blood flow imaging by a swept laser source-based Fourier domain optical Doppler tomography. Optics Express. 2005;**13**(19):7449-7457

[16] Spaide RF, Koizumi H, Pozzoni MC. Enhanced depth imaging spectral-domain optical coherence tomography. American Journal of Ophthalmology. 2008;**146**(4):496-500

[17] Walsh AC. Binocular optical coherence tomography. Ophthalmic Surgery, Lasers & Imaging. 2011;**42**(Suppl):S95-s105

[18] Jia Y, Tan O, Tokayer J, Potsaid B, Wang Y, Liu JJ, et al. Split-spectrum amplitude-decorrelation angiography with optical coherence tomography. Optics Express. 2012;**20**(4):4710-4725

[19] Reif R, Qin J, An L, Zhi Z, Dziennis S, Wang R. Quantifying optical microangiography images obtained from a spectral domain optical coherence tomography system. International Journal of Biomedical Imaging. 2012;**2012**:509783

[20] Choi W, Mohler KJ, Potsaid B, Lu CD, Liu JJ, Jayaraman V, et al. Choriocapillaris and choroidal microvasculature imaging with ultrahigh speed OCT angiography. PLoS One. 2013;**8**(12):e81499

[21] Spaide RF, Fujimoto JG, Waheed NK, Sadda SR, Staurenghi G. Optical coherence tomography angiography. Progress in Retinal and Eye Research. 2018;**64**:1-55

[22] Zhang A, Zhang Q, Wang RK. Minimizing projection artifacts for accurate presentation of choroidal neovascularization in OCT micro-angiography. Biomedical Optics Express. 2015;**6**(10):4130-4143

[23] Liu L, Gao SS, Bailey ST, Huang D, Li D, Jia Y. Automated choroidal neovascularization detection algorithm for optical coherence tomography angiography. Biomedical Optics Express. 2015;**6**(9):3564-3576

[24] Yoshikawa YST, Kanno J, Kimura I, Hangai M, Shinoda K. Optic disc vessel density in nonglaucomatous and glaucomatous eyes: An enhanced-depth imaging optical coherence tomography angiography study. Clinical Ophthalmology. 2018;**12**:1113-1119

[25] Le PH, Patel BC. Optical Coherence Tomography Angiography. Treasure Island (FL): StatPearls; 2022

[26] Browning DJ, Glassman AR, Aiello LP, Bressler NM, Bressler SB, Danis RP, et al. Optical coherence tomography measurements and analysis methods in optical coherence tomography studies of diabetic macular edema. Ophthalmology. 2008;**115**(8):1366-1371, 71.e1

[27] Bhende M, Shetty S, Parthasarathy M, Ramya S. Optical coherence tomography: A guide to interpretation of common macular diseases. Indian Journal of Ophthalmology. 2018;**66**(1):20-35

[28] Nesper PL, Fawzi AA. Human Parafoveal capillary vascular anatomy and connectivity revealed by optical coherence tomography angiography. Investigative Ophthalmology & Visual Science. 2018;**59**(10):3858-3867

[29] Jia Y, Wei E, Wang X, Zhang X, Morrison JC, Parikh M, et al. Optical coherence tomography angiography of optic disc perfusion in glaucoma. Ophthalmology. 2014;**121**(7):1322-1332

[30] Chen CL, Bojikian KD, Gupta D, Wen JC, Zhang Q, Xin C, et al. Optic nerve head perfusion in normal eyes and eyes with glaucoma using optical coherence tomography-based microangiography. Quantitative Imaging in Medicine and Surgery. 2016;**6**(2):125-133

[31] Andrade De Jesus D, Sánchez Brea L, Barbosa Breda J, Fokkinga E, Ederveen V, Borren N, et al. OCTA multilayer and multisector Peripapillary microvascular modeling for diagnosing and staging of

glaucoma. Translational Vision Science & Technology. 2020;**9**(2):58

[32] Bekkers A, Borren N, Ederveen V, Fokkinga E. Andrade De Jesus D, Sánchez Brea L, et al. microvascular damage assessed by optical coherence tomography angiography for glaucoma diagnosis: A systematic review of the most discriminative regions. Acta Ophthalmologica. 2020;**98**(6):537-558

[33] Eslami Y, Ghods S, Mohammadi M, Safizadeh M, Fakhraie G, Zarei R, et al. The role of optical coherence tomography angiography in moderate and advanced primary open-angle glaucoma. International Ophthalmology. 2022;**42**(12):3645-3659

[34] Mohammadzadeh V, Fatehi N, Yarmohammadi A, Lee JW, Sharifipour F, Daneshvar R, et al. Macular imaging with optical coherence tomography in glaucoma. Survey of Ophthalmology. 2020;**65**(6):597-638

[35] Takusagawa HL, Liu L, Ma KN, Jia Y, Gao SS, Zhang M, et al. Projection-resolved optical coherence tomography angiography of macular retinal circulation in glaucoma. Ophthalmology. 2017;**124**(11):1589-1599

[36] Kim J-A, Lee EJ, Kim T-W. Evaluation of parapapillary choroidal microvasculature dropout and progressive retinal nerve fiber layer thinning in patients with glaucoma. JAMA Ophthalmology. 2019;**137**(7):810-816

[37] Chatziralli I, Milionis I, Christodoulou A, Theodossiadis P, Kitsos G. The role of vessel density as measured by optical coherence tomography angiography in the evaluation of Pseudoexfoliative glaucoma: A review of the literature. Ophthalmol Ther. 2022;**11**(2):533-545

[38] Chen HS, Liu CH, Wu WC, Tseng HJ, Lee YS. Optical coherence tomography angiography of the superficial microvasculature in the macular and Peripapillary areas in glaucomatous and healthy eyes. Investigative Ophthalmology & Visual Science. 2017;**58**(9):3637-3645

[39] Geyman LS, Garg RA, Suwan Y, Trivedi V, Krawitz BD, Mo S, et al. Peripapillary perfused capillary density in primary open-angle glaucoma across disease stage: An optical coherence tomography angiography study. The British Journal of Ophthalmology. 2017;**101**(9):1261-1268

[40] Bowd C, Belghith A, Rezapour J, Christopher M, Hyman L, Jonas JB, et al. Diagnostic accuracy of macular thickness map and texture En face images for detecting glaucoma in eyes with axial high myopia. American Journal of Ophthalmology. 2022;**242**:26-35

[41] Suwan Y, Fard MA, Geyman LS, Tantraworasin A, Chui TY, Rosen RB, et al. Association of Myopia with Peripapillary perfused capillary density in patients with glaucoma: An optical coherence tomography angiography study. JAMA Ophthalmology. 2018;**136**(5):507-513

[42] Chang PY, Wang JY, Wang JK, Huang TL, Hsu YR. Optical coherence tomography angiography compared with optical coherence tomography for detection of early glaucoma with high myopia. Front Med (Lausanne). 2021;**8**:793786

[43] Shin JW, Kwon J, Lee J, et al. Relationship between vessel density and visual field sensitivity in glaucomatous eyes with high myopia. The British Journal of Ophthalmology. 2019;**103**:585-591

[44] Yilmaz H, Yeşiltaş YS, Aydemir E, Aksoy Aydemir G, Gökgöz Özışık G,

Koylu MT, et al. A myopic normative database for retinal nerve fiber layer thickness using optical coherence tomography. Journal of Glaucoma. 2022;**31**(10):816-825

[45] Protsyk O, Gallego-Pinazo R, Dolz-Marco R. Limitaciones actuales y futuro de la angiografía por tomografía de coherencia óptica. Archivos de la Sociedad Española de Oftalmología. 2022;**97**(8):421-423

[46] Anvari P, Ashrafkhorasani M, Habibi A, Falavarjani KG. Artifacts in optical coherence tomography angiography. J. Ophthalmic Vis. Res. 2021;**16**(2):271-286

[47] Kamalipour A, Moghimi S, Hou H, Penteado RC, Oh WH, Proudfoot JA, et al. OCT angiography artifacts in glaucoma. Ophthalmology. 2021;**128**(10):1426-1437

[48] Cheng W, Song Y, Lin F, Xiong J, Li F, Jin L, et al. Assessment of artifacts in swept-source optical coherence tomography angiography for glaucomatous and Normal eyes. Translational Vision Science & Technology. 2022;**11**(1):23

[49] PKP M, Patel M, Kim-Cavdar KKS, editors. OCT-A artifacts in healthy, ocular hypertension, glaucoma suspect, myopic and glaucomatous eyes. In: American Academy of Ophthalmology Annual Meeting. Chicago, IL; 2022

[50] Weijing C, Zhang X, Wang W. Artifacts associated with swept-source OCT-angiography measurements in glaucoma. Investigative Ophthalmology & Visual Science. 2020;**61**(7):4117

[51] Ferguson RD, Hammer DX, Paunescu LA, Beaton S, Schuman JS. Tracking optical coherence tomography. Optics Letters. 2004;**29**(18):2139-2141

[52] Venugopal JP, Rao HL, Weinreb RN, Dasari S, Riyazuddin M, Pradhan ZS, et al. Repeatability and comparability of peripapillary vessel density measurements of high-density and non-high-density optical coherence tomography angiography scans in normal and glaucoma eyes. The British Journal of Ophthalmology. 2019;**103**(7):949-954

[53] Manalastas PIC, Zangwill LM, Saunders LJ, Mansouri K, Belghith A, Suh MH, et al. Reproducibility of optical coherence tomography angiography macular and optic nerve head vascular density in glaucoma and healthy eyes. Journal of Glaucoma. 2017;**26**(10):851-859

[54] Munk MR, Kashani AH, Tadayoni R, Korobelnik JF, Wolf S, Pichi F, et al. Standardization of OCT angiography nomenclature in retinal vascular diseases: First survey results. Ophthalmol Retina. 2021;**5**(10):981-990

[55] Sampson DM, Dubis AM, Chen FK, Zawadzki RJ, Sampson DD. Towards standardizing retinal optical coherence tomography angiography: A review. Light: Science & Applications. 2022;**11**(1):63

[56] Janiesch C, Zschech P, Heinrich K. Machine learning and deep learning. Electronic Markets. 2021;**31**(3):685-695

[57] Le D, Son T, Yao X. Machine learning in optical coherence tomography angiography. Experimental Biology and Medicine (Maywood, N.J.). 2021;**246**(20):2170-2183

[58] Hormel TT, Hwang TS, Bailey ST, Wilson DJ, Huang D, Jia Y. Artificial intelligence in OCT angiography. Progress in Retinal and Eye Research. 2021;**85**:100965

[59] Chan YM, Ng EYK, Jahmunah V, Wei Koh JE, Lih OS, Wei Leon LY, et al.

Automated detection of glaucoma using optical coherence tomography angiogram images. Computers in Biology and Medicine. 2019;**115**:103483

[60] Kooner KS, Angirekula A, Treacher AH, Al-Humimat G, Marzban MF, Chen A, et al. Glaucoma diagnosis through the integration of optical coherence tomography/angiography and machine learning diagnostic models. Clinical Ophthalmology. 2022;**16**:2685-2697

[61] Bowd C, Belghith A, Zangwill LM, Christopher M, Goldbaum MH, Fan R, et al. Deep learning image analysis of optical coherence tomography angiography measured vessel density improves classification of healthy and glaucoma eyes. American Journal of Ophthalmology. 2022;**236**:298-308

[62] Sreejith Kumar AJ, Chong RS, Crowston JG, Chua J, Bujor I, Husain R, et al. Evaluation of generative adversarial networks for high-resolution synthetic image generation of Circumpapillary optical coherence tomography images for glaucoma. JAMA Ophthalmol. 2022;**140**(10):974-981

[63] Yamashita K, Markov K, editors. Medical image enhancement using super resolution methods. In: Computational Science–ICCS 2020. Cham: Springer International Publishing;

[64] Omodaka K, Horie J, Tokairin H, Kato C, Ouchi J, Ninomiya T, et al. Deep learning-based noise reduction improves optical coherence tomography angiography imaging of radial Peripapillary capillaries in advanced glaucoma. Current Eye Research. 2022;**47**(12):1600-1608

[65] Hemelings R, Elen B, Barbosa-Breda J, Blaschko MB, De Boever P, Stalmans I. Deep learning on fundus images detects glaucoma beyond the optic disc. Scientific Reports. 2021;**11**(1):20313